Click Here for Full Article

Interannual variability of evapotranspiration and energy exchange over an annual grassland in California

Youngryel Ryu,[1] Dennis D. Baldocchi,[1] Siyan Ma,[1] and Ted Hehn[1]

[1]   We report on the interannual variability of evapotranspiration (E) and energy exchange of an annual grassland in the Mediterranean climate zone of California. They were measured directly with the eddy covariance technique over a 6-year period that spanned between July 2001 and June 2007 and experienced a large range in precipitation (376 mm to 888 mm). Despite a two-fold range in precipitation, annual E ranged much less, between 266 mm and 391 mm. We found that pronounced energy-limited and water-limited periods occurred within the same year. In the water-limited period, monthly integrated E scaled negatively with solar radiation and was restrained by precipitation. In the energy-limited period, on the other hand, the majority of E scaled positively with solar radiation (R_g) and was confined by potential E (E_p). E was most sensitive to the availability of soil moisture during the transition to the senescence period rather than onset of the greenness period, causing annual E to be strongly modulated by growing season length. Bulk surface conductance scaled consistently with Priestley-Taylor α coefficient regardless of interannual and seasonal variability of precipitation, E, and solar radiation.

Citation: Ryu, Y., D. D. Baldocchi, S. Ma, and T. Hehn (2008), Interannual variability of evapotranspiration and energy exchange over an annual grassland in California, *J. Geophys. Res.*, *113*, D09104, doi:10.1029/2007JD009263.

1.   Introduction

[2]   Evidence of global climate change is well-documented, with long-term increases observed in average global surface temperature [*Houghton et al.*, 2001; *Jones and Moberg*, 2003], the atmosphere's carbon dioxide (CO_2) concentration [*Keeling et al.*, 1996], precipitation [*Dai et al.*, 1997; *Hulme et al.*, 1998], and runoff [*Gedney et al.*, 2006; *Groisman et al.*, 2004; *Labat et al.*, 2004]. However, there are still several unresolved critical issues relating to climate change. One issue is whether evapotranspiration (E) is increasing or decreasing. Even though there is general consensus that precipitation and runoff have increased [*Dai et al.*, 1997; *Gedney et al.*, 2006], the trend for E is still being debated. One may expect hydrological intensification and greater E with global warming [*Huntington*, 2006], but there are many positive and negative feedbacks in play.

[3]   Some scientists argue that E has increased and has contributed to hydrological intensification [*Brutsaert*, 2006; *Golubev et al.*, 2001; *Wetherald and Manabe*, 2002], while others argue that global dimming, caused by anthropogenic pollutants, has caused E to decrease and such dimming has dampened the water cycle [*Liepert et al.*, 2004; *Liu et al.*, 2004; *Ramanathan et al.*, 2001; *Roderick and Farquhar*, 2002a; *Wild et al.*, 2004]. This lack of consensus stems in part from a lacking of direct and long-term measurements of actual E. The majority of E measurements associated with this debate have been derived from pan E, which does not measure actual E [*Morton*, 1978].

[4] E is considered the most problematic term in the hydrological budget [*Lettenmaier and Famiglietti*, 2006]. It is generally evaluated as the residual between precipitation and runoff in the regional scale and as the residual between precipitation, runoff and interception at the catchment scale [*Bosch and Hewlett*, 1982; *Jaeger and Kessler*, 1997; *Lewis et al.*, 2000; *Marc and Robinson*, 2007]. It is also estimated by measuring pan E [*Brutsaert and Parlange*, 1998; *Brutsaert*, 2006; *Ohmura and Wild*, 2002; *Peterson et al.*, 1995; *Roderick and Farquhar*, 2002b]. Indirect measures of E lack mechanistic information on biophysical processes, which include stomatal and boundary layer conductances and leaf area index. Better and long-term information on E from direct measurements is needed to better understand complex feedbacks between the terrestrial biosphere and climate system, for managing water resources, monitoring floods and droughts, and estimating the land surface energy balance that controls the height of the planetary boundary layer, climate and land-atmosphere feedback [*Brubaker and Entekhabi*, 1996; *Raupach*, 1998].

[5]   The eddy covariance method provides a direct means of measuring E [*Wilson and Baldocchi*, 2000]. Because of its relatively short history, long-term studies using the eddy covariance technique are relatively rare compared to pan E. Five or more years of data on CO_2, water vapor, and energy exchange have been collected for the following

[1]Ecosystem Science Division, Department of Environmental Science, Policy and Management, University of California at Berkeley, Berkeley, California, USA.

ecosystems: boreal forests [*Arain et al.*, 2002; *Barr et al.*, 2007; *Dunn et al.*, 2007], temperate deciduous forests [*Barford et al.*, 2001; *Carrara et al.*, 2003; *Hanson et al.*, 2004; *Wilson and Baldocchi*, 2001], savannas [*Beringer et al.*, 2007; *Ma et al.*, 2007], a steppe [*Gilmanov et al.*, 2006], a subalpine forest [*Monson et al.*, 2005], a shrub ecosystem [*Luo et al.*, 2007], a northern peatland [*Roulet et al.*, 2007], spruce forests [*Grunwald and Bernhofer*, 2007; *Hollinger et al.*, 2004], and a mixture of agricultural fields and forested patches [*Haszpra et al.*, 2005]. While all of the cited papers measure water vapor exchange, most focus on CO_2 exchange. To our knowledge, there are only a few publications covering more than five years for E measurement explicitly, namely in a temperate deciduous forest [*Hanson et al.*, 2004], a spruce forest [*Grunwald and Bernhofer*, 2007], a bog [*Lafleur et al.*, 2005], a chaparral [*Luo et al.*, 2007], and boreal forests [*Arain et al.*, 2002; *Barr et al.*, 2007]. Another cohort of studies have reported interannual variability of ET for less than five years in temperate deciduous forests [*Moore et al.*, 1996; *Wilson and Baldocchi*, 2000], boreal forests [*Amiro et al.*, 2006; *Arain et al.*, 2003], a cypress forest [*Kosugi et al.*, 2007], a lake [*Rouse et al.*, 2003], a tallgrass prairie [*Burba and Verma*, 2005], a grassland [*Jacobs et al.*, 2007], an Amazonian rain forest [*Hutyra et al.*, 2007], a maize-soybean agricultural system [*Suyker and Verma*, 2007], and a savanna [*Baldocchi et al.*, 2004]. The eddy covariance method is susceptible to errors when the surface energy balance does not close and the flux tower is located on non-ideal terrain (e.g., rugged or heterogeneous landscapes) [*Wilson et al.*, 2002]. Its strengths, however, are in measuring interannual variability because bias errors tend to be constant from year to year.

[6] Grasslands cover 20% of global land area [*Wang et al.*, 2006a]. They are of particular interest because it is not certain how water yield changes under land conversion from grassland to forest and vice versa [*Marc and Robinson*, 2007], and their water vapor and CO_2 exchange is expected to respond to climate perturbations more sensitively (e.g., drought and extreme heavy rain event) [*Knapp and Smith*, 2001; *Knapp et al.*, 2002; *Parton et al.*, 1994]. Grassland E studies have been performed in the Great Plains of North America [*Bremer et al.*, 2001; *Burba and Verma*, 2001, 2005; *Ham and Knapp*, 1998; *Kim and Verma*, 1990; *Meyers*, 2001; *Verma et al.*, 1989, 1992], over a mixed grassland in Canada [*Wever et al.*, 2002], a warm-temperate grassland in southeastern USA [*Novick et al.*, 2004], a grass field [*Saigusa et al.*, 1998] and a wet temperate grassland [*Li et al.*, 2005] in Japan, a tussock grassland in New Zealand [*Hunt et al.*, 2002], a C_4 pasture in Brazil [*Grace et al.*, 1998], and a perennial grassland in Netherlands [*Jacobs et al.*, 2007]. The majority of these studies were conducted over relatively short periods, such as one year or less. Only two studies exist on E from the annual grasslands in a Mediterranean-type climate. One was for four months near the Pacific coast range of California [*Valentini et al.*, 1995] and the other was for two years on the foothills of the Sierra Nevada mountains at the present study site [*Baldocchi et al.*, 2004].

[7] An annual grassland, growing in a Mediterranean-type climate in California, is unique from other grassland ecosystems because it has a different phenological cycles.

The grasses live from November to May, during the winter rainy season and are dead during the summer months [*Biswell*, 1956; *Parton et al.*, 1994; *Pitt and Heady*, 1978]. Because the wet winter season receives the least solar radiation with the most rainfall, the water supply, precipitation, exceeds atmospheric demand for water, potential E (E_p). However, during the dry season, grasslands receive the highest solar radiation with least rainfall, causing the potential water demand to greatly exceed water supply. Budyko's aridity index (AI) is given as the ratio of precipitation to E_p and is widely used to determine whether a region is water-limited (AI < 1) or energy-limited (AI > 1) [*Baldocchi and Xu*, 2007; *Budyko*, 1974; *Donohue et al.*, 2007; *Farquhar and Roderick*, 2007; *Yang et al.*, 2006]. This ecosystem is relatively unique because it undergoes both pronounced water-limited and energy-limited periods in the same year. Consequently, the study of intraannual variability of E can help understand which period influences annual E most and how the timing of transition from energy-limited to water-limited modulates the annual E amount. Furthermore, because this ecosystem experiences large interannual variability in precipitation (376 mm to 888 mm per year during the study period), it is critical to understand how E is downregulated with soil water deficits.

[8] Here, we report on six hydrological years of E and energy exchanges over an annual grassland growing in the Mediterranean-type climate of California. Direct measurements of E were made with the eddy covariance method between July 2001 to June 2007. The objectives of this study include: 1) to characterize E, energy fluxes and related bulk parameters (e.g., surface conductance, decoupling factor and Priestley-Taylor α coefficient) in monthly and annual timescales, and 2) to investigate which abiotic and biotic factors control the interannual variability of water and energy fluxes. Additionally, we will use our data to address questions related to E biogeography for classifying plant functional type (PFT). The scientific questions to be addressed in this study include: (1) how will growing season length influence annual E amount?; (2) How does the timing of transition from energy-limited to water-limited modulate annual ET amount?; (3) Which factors control E-atmospheric demand or stomatal regulation?; and (4) How does E respond to changes in solar radiation amounts in water-limited and energy-limited periods?

2. Materials and Methods

2.1. Site Description

[9] The study site is a member of the AmeriFlux network and is classified as a grazed annual grassland in central California, USA (Vaira Ranch, latitude: 38.4133°N; longitude: 120.9508°W; altitude: 129 m). It is located on the lower foothills of the Sierra Nevada Mountains. It experiences a Mediterranean-type climate with dry hot summers and wet mild winters. Rainfall is concentrated between November and May with little precipitation during the summer. Climate data show that the annual average temperature and annual precipitation amount are 16.9°C and 565 mm, respectively (1949 to 2005 data from the Camp Pardee, CA climate station, which is at a similar altitude and is 26 km south of the study site: http://www.wrcc.dri.edu/cgi-bin/cliMAIN.pl?cacamp+nca). The soil is an Exchequer

Table 1. Annual Energy Balance Closure for Linear Regression Coefficients and the Ratio of $\lambda E + H + G$ to R_n

Year[a]	Slope	Intercept (W m^{-2})	r^2	$(\lambda E^{\text{b}} + H^{\text{c}} + G^{\text{d}})/R_n^{\text{e}}$
01–02	0.90	2.11	0.97	0.92
02–03	0.90	4.03	0.98	0.95
03–04	0.86	7.10	0.97	0.94
04–05	0.81	15.25	0.97	1.02
05–06	0.88	18.84	0.97	1.12
06–07	0.87	14.21	0.97	1.04

[a]Year was defined as hydrological year (e.g., July to June). 01–02 indicates July 2001 to June 2002.
[b]λE: latent heat flux.
[c]H: sensible heat flux.
[d]G: soil heat flux.
[e]R_n: net radiation.

very rocky silt loam (Lithic xerorthents), which is composed of 30% sand, 57% silt and 13% clay. The bulk density at the surface layer (0–30 cm) is 1.43 ± 0.10 g cm^{-3}. The soil profile is about 0.5 m depth with overlaying fractured rock. The site is dominated by the cool-season C_3 annual species, including *Brachypodium distachyon* L., *Hypochaeris glabra* L., *Trifolium dubium* Sibth., *Trifolium hirtum* All., *Dichelostemma volubile* A., and *Erodium botrys* Cav. More detailed site information may be found in previous studies [*Baldocchi et al.*, 2004; *Xu and Baldocchi*, 2004].

2.2. Data Acquisition

[10] Water vapor, CO_2, energy fluxes and meteorological variables have been measured since November 2000. The eddy covariance system is composed of a triaxial sonic anemometer (Model 1352, Gill Instruments Ltd., Lymington, England) and an open-path fast response infrared gas analyzer (IRGA, Li 7500, Li-Cor Inc., Lincoln, NE, USA). The sensors were mounted at 2 m height above the ground. The fetch from all direction was over 200 m and only a few sparse oak trees were within the footprint area [*Kim et al.*, 2006]. Radiation flux densities were measured at 2.5 m height with an upward and downward facing quantum sensor (PAR Like, Kipp and Zonen, Delft, Netherlands), a net radiometer (NR Lite, Kipp and Zonen, Delft, Netherlands) and a pyranometer (CM11, Kipp and Zonen, Delft, Netherlands). Air temperature and relative humidity were measured at 2.5 m height with a shielded and aspirated sensor (HMP-35 A, Vaisala, Helsinki, Finland). Soil volumetric water content was measured at the depths of 0.05, 0.1, and 0.2 m with frequency domain reflectometry sensor (ML2-X, Delta-T Devices, Cambridge, UK). Green leaf area index (L_G) was determined by harvesting four sample plots (0.25 m × 0.25 m) within the footprint of flux tower when the grass was living. The dates of grass germination and senescence were detected based on the extrapolation of data obtained during periodic field visits (weekly to biweekly). The growing season length was calculated from these values [*Ma et al.*, 2007]. Additional details on the data acquisition are available in previous papers [*Baldocchi et al.*, 2004; *Xu and Baldocchi*, 2004].

2.3. Gap Filling, Assessing Uncertainty, and Data Processing

[11] Data gaps are unavoidable in long-term and continuous measurements. We filled short data gaps (<3 h) with linear interpolation and we used the mean diurnal method for filling longer gaps [*Falge et al.*, 2001]. The diurnal means were calculated for 26 consecutive day windows, which correspond well with a spectral gap in energy fluxes in the site [*Baldocchi et al.*, 2004]. For periods with missing solar radiation, air temperature and precipitation data, we used the measurements from the nearby companion site (Tonzi Ranch, 2 km away). We compared numerous meteorological variables between the two sites and found that they were interchangeable. For assessing the data quality, we analyzed the linear regressions of the sum of latent heat (λE), sensible heat (H) and soil heat flux densities (G) against the net radiation (R_n). The half hourly data, which excluded gap filled data, were used to perform the linear regression analysis. The annual sum of $\lambda E + H + G$ divided by annual sum of R_n is presented in Table 1. In general, energy balance closure on annual timescales ranged between 0.92 and 1.12 with an average of 1.00. Although not perfect, our ability to close the surface energy was better than the average energy closure across FLUXNET sites for shorter term periods (0.80) [*Wilson et al.*, 2002] and was comparable to the comprehensive studies over short vegetation [*Heusinkveld et al.*, 2004; *Meyers and Hollinger*, 2004].

[12] For quantifying uncertainties associated with the annual sum of E, we used the bootstrap technique with the Monte Carlo approach [*Efron and Tibshirani*, 1993]. It estimates bias, standard error, confidence interval or prediction intervals. In prior studies, it has been used to assess uncertainties of gross primary production [*Hagen et al.*, 2006; *Ma et al.*, 2007]. We assessed the uncertainty of each annual E sum at the 90% confidence interval. The confidence intervals for annual E are shown in Table 2.

[13] In order to distill and interpret the large amount of information collected over six years, we relied on and presented monthly averages of daily sums of solar radiation (R_g), R_n, λE, H, and G. *Baldocchi et al.* [2001b] reported that there is a pronounced spectral gap in E and CO_2 exchange at the monthly scale, making it an appropriate time step to capture seasonal and phenological change. This time step is also used in other interannual studies on E [*Arain et al.*, 2002; *Lafleur et al.*, 2005]. In analyzing annual sums of E and meteorology, we used the hydrological year, defined as the period from July of current year to June of next year (e.g., 03–04 is from July 2003 to June 2004). This is standard practice for hydrological analyzes in California because it was necessary to include the entire rainy season (November to May) into one year.

2.4. Calculations of Bulk Parameters

[14] To interpret the interannual variability of E and energy fluxes, we used three model parameters: bulk surface conductance [*Monteith*, 1965], decoupling factor [*Jarvis and McNaughton*, 1986], and the Priestley-Taylor α coefficient [*Priestley and Taylor*, 1972].

[15] The bulk surface conductance (G_s) is related to the weighted integration of individual leaf's conductance [*Baldocchi and Meyers*, 1998; *Raupach*, 1995] and it was computed by inverting from the Penman-Monteith equation:

$$\frac{1}{G_s} = \frac{1}{G_a}\left\{\frac{\varepsilon(R_n - G) + \rho C_p G_a D/\gamma}{\lambda E} - \varepsilon\right\} - 1 \quad (1)$$

Table 2. Summary of Energy Fluxes, Climatology, and Bulk Parameters for the 6-Year

Variable	Year						
	01−02	02−03	03_04	04−05	05−06	06−07	Avg
Solar radiation (GJ m^{-2})	6.69	6.55	6.70	6.40	6.50	6.89	6.62
Net radiation (GJ m^{-2})	2.18	2.28	2.46	2.08	2.15	2.14	2.21
Latent heat flux (GJ m^{-2})	0.72	0.79	0.66	0.96	0.85	0.75	0.79
Sensible heat flux (GJ m^{-2})	1.34	1.39	1.66	1.33	1.60	1.55	1.48
Soil heat flux (GJ m^{-2})	0.00	0.01	0.1	0.01	0.09	0.05	0.04
% flux data coverage	59	77	76	62	79	78	72
Temperature (°C)	15.5	15.6	16.3	15.3	16.1	15.8	15.8
Vapor pressure deficit (kPa)	0.99	1.03	1.10	0.88	1.01	1.09	1.02
Precipitation (mm)	500	491	407	704	888	376	561
Evapotranspiration (mm)	292 (±25)[a]	319 (±28)	266 (±25)	391 (±33)	343 (±29)	303 (±28)	319 (±28)
Potential evaporation (mm)	879	954	1049	950	977	959	961
α (year)[b]	0.47	0.48	0.34	0.53	0.44	0.42	0.45
α (growing season)[c]	0.89	0.87	0.67	0.87	0.82	0.79	0.82
G_s[d] (mm sec^{-1}) (year)	4.01	4.74	2.77	5.79	4.29	3.27	4.14
G_s (mm sec^{-1})(growing season)	9.01	10.08	5.95	11.02	8.89	6.96	8.65
Ω[e] (year)	0.27	0.29	0.22	0.32	0.26	0.23	0.27
Ω (growing season)	0.55	0.57	0.46	0.57	0.50	0.44	0.51
Growing season length (days)	154	172	143	214	165	176	171
Max LAI	2.6	2.6	2.2	2.7	1.9	2.6	2.4

[a]The parenthesis indicates 90% of confidence interval estimated from bootstrap technique.
[b]Priestley-Taylor α coefficient.
[c]Growing season indicates from January to April.
[d]Bulk surface conductance.
[e]Decoupling factor.

where ρ is air density (kg m^{-3}), C_p is specific heat capacity of air (J kg^{-1} K^{-1}), ε is s/γ, s is the slope of relation between saturation vapor pressure and temperature, γ is psychrometric constant, D is vapor pressure deficit (kPa) and G_a is bulk aerodynamic conductance. G_a was calculated as follows:

$$R_a = R_{a,m} + R_b \quad (2)$$

$$R_{a,m} = u/u_*^2 \quad (3)$$

$$R_b = kB^{-1}/ku_* \quad (4)$$

where R_a (bulk aerodynamic resistance) is a reciprocal of G_a, $R_{a,m}$ is aerodynamic resistance for momentum transfer, R_b is quasi-laminar boundary layer resistance [*Thom*, 1972], k is von Karman constant (0.4), u_* is friction velocity, which was measured directly with the eddy covariance system. The structure of the land surface determines kB^{-1}. In this case, a value of 2 was used because it is a representative value for the dense grass canopies [*Garratt and Hicks*, 1973; *Verma*, 1989].

[16] The decoupling factor (Ω) explains the degree of coupling between vegetation and atmosphere. It ranges from 0 when **E** is controlled by G_s and vapor pressure deficit to 1 when **E** is controlled by the available energy [*Jarvis and McNaughton*, 1986]. It was calculated as follows:

$$\Omega = \frac{\varepsilon + 1}{\varepsilon + 1 + \dfrac{G_a}{G_s}} \quad (5)$$

The Priestley-Taylor α coefficient represents the ratio between measured **λE** and equilibrium evaporation (**λE**$_{eq}$)

$$\alpha = \frac{\lambda E}{\lambda E_{eq}} \quad (6)$$

where **λE**$_{eq}$ is equilibrium **λE**: $\frac{(R_n - G)s}{s+\gamma}$. It provides a comparison of measured **λE** to a climatologically expected

λE assuming a closed volume with constant net radiation over a wet surface [*McNaughton and Spriggs*, 1986]. Potential **λE** was calculated from $1.26 \times$ **λE**$_{eq}$ [*Priestley and Taylor*, 1972].

[17] To avoid the numerical instability that occurs when the denominator approaches zero, only daytime data of G_s, Ω and α (10:00 to 14:00) were used to calculate the monthly mean values.

3. Results

3.1. General Weather Conditions and Phenology

[18] The average annual air temperature during the 6-year period was 15.8°C with the minimum of 15.3°C in the 04−05 hydrological year and maximum of 16.3°C in the 03−04 hydrological year (Table 2). The monthly average of the daily maximum air temperature (T_x) ranged from 10°C to 20°C in the wet seasons and reached extreme levels (~35°C) in the dry seasons (Figure 1a). The monthly average of the daily minimum air temperature (T_n) remained positive, indicating that the site did not experience prolonged periods of freezing (Figure 1a). The ecosystem experienced a wide diurnal temperature difference (i.e., T_x minus T_n), which ranged from 20°C during the dry seasons when the grass was dead to 10°C in the wet seasons when the grass actively transpired. The annual precipitation showed large interannual variation. It ranged between 376 mm (06−07 hydrological year) and 888 mm (05−06 hydrological year), producing an average and standard deviation of 561 mm and 198 mm, respectively (Figure 1b). The monthly precipitation showed that the 04−05 hydrological year experienced the longest wet season ranging from October to June, whereas the 03−04 hydrological year underwent the shortest wet season from November to March (Figure 1b). Because of the Mediterranean-type climate, over 90% of annual precipitation fell during the November to April wet season. The soil profile experienced extremely dry conditions during the summer,
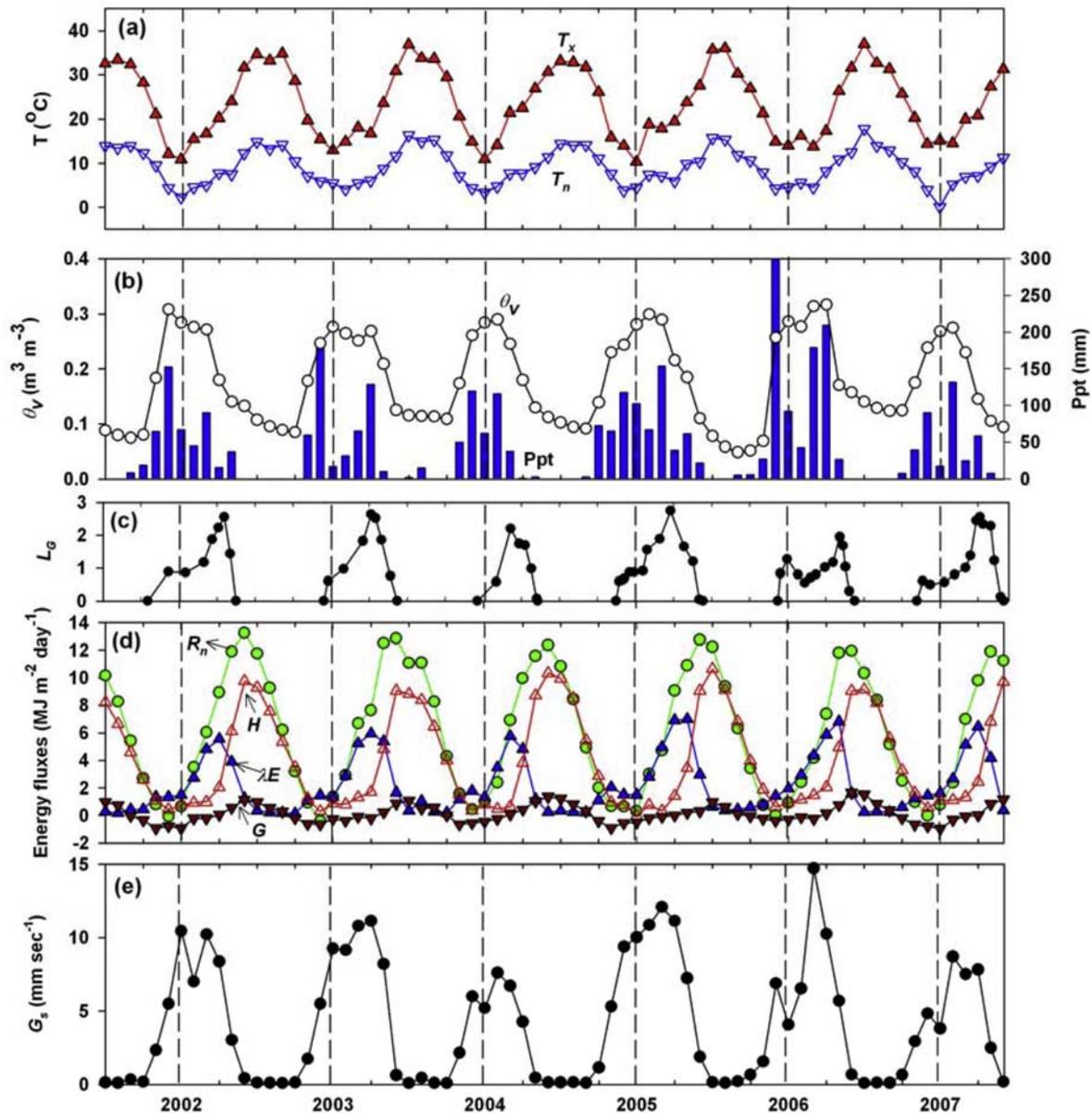
Figure 1. (a) Monthly average of daily maximum (T_x) and minimum (T_n) air temperature. (b) Monthly average of volumetric soil water content at 5-cm depth (θ_v), and monthly sum of precipitation (Ppt). (c) Green leaf area index (L_G). L_G was measured periodically so it is marked in daily scale on the graph. (d) Monthly average of daily integrated net radiation (R_n), latent heat flux (λE), sensible heat flux (H), and soil heat flux (G). (e) Monthly average of bulk surface conductance (G_s).

and soil moisture was recharged by the winter rainfall (Figure 1b). L_G showed that winter rainfall triggered slow vegetation growth, which accelerated in spring due to the availability of ample soil moisture and which reached maximum values in April or May (Figure 1c). The maximum growth period did not last very long, and the grass quickly senesced in response to the subsequent soil moisture deficits and high air temperatures.

3.2. PAR Albedo

[19] The monthly trends in the albedo of photosynthetically active radiation (PAR albedo) are shown in Figure 2a. The PAR albedo is related to plant greenness rather than

energy availability because reflected near infrared radiation is missing. The canopy growth is related to the radiation absorption, particularly PAR [*Burba and Verma*, 2001; *Monteith and Unsworth*, 1990; *Song*, 1999]. The monthly PAR albedos showed a clear seasonal pattern with the annual average ranging between 0.102 and 0.124. In general, PAR albedo decreased abruptly in November and December due to the start of rainfall and greenness. It reached its minimum values (between 0.05 and 0.08) in April. Afterward, PAR albedo quickly increased with the start of senescence. The PAR albedo showed the earliest onset of growing season (i.e., the lowest PAR albedo in November and December) and the latest senescence
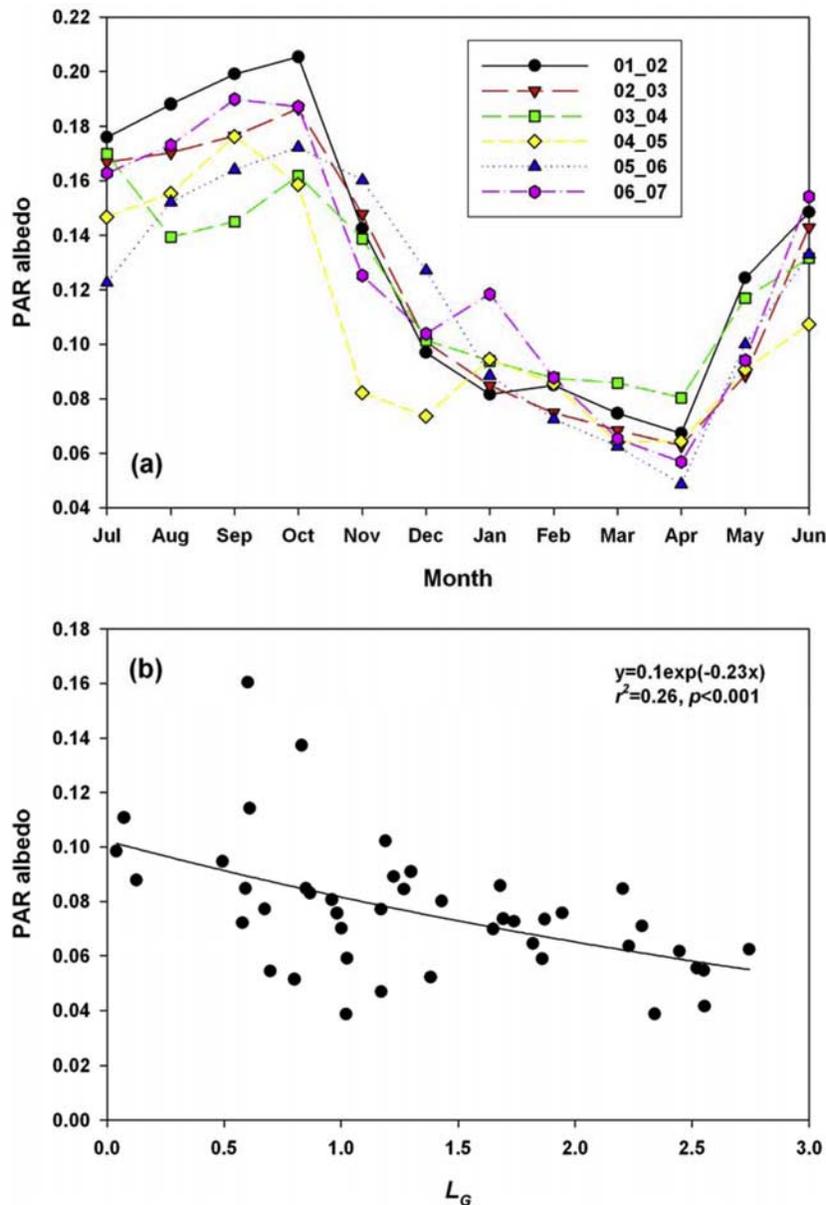
Figure 2. (a) Monthly average of daily PAR albedo for the 6-year period. Monthly average was calculated from the ratio of the sum of outgoing PAR to the sum of incoming PAR for each month. 01–02 indicates July 2001 to June 2002. (b) The relationships between green leaf area index (L_G) and PAR albedo during the growing seasons. PAR albedos are daily average values from 10:00 to 14:00.

(i.e., the lowest PAR albedo in June) in the 04–05 hydrological year. This observation is consistent with the fact that that year had the longest growing season. The PAR albedo scaled negatively with L_G, implying that PAR albedo can capture phenological events and canopy structure (Figure 2b) well. In August of the 03–04 hydrological year, the PAR albedo decreased abruptly in contrast to the other years because of an uncommon summer rainfall event (Figure 1).

3.3. Radiation and Energy Flux Densities

[20] The average annual integral of shortwave radiation, R_g, during the 6-year period was 6.62 GJ m^{-2}. During the dry season, R_g showed the similar pattern, year to

year, because the skies tend to be cloudless. High interannual variations are attributed to levels of cloudiness during in the wet seasons, which affects rainfall, too (Figure 3a).

[21] The averaged annually integrated net radiation balance, R_n, over 6-year was 2.21 GJ m^{-2}. This value is about 33% of annual R_g (6.62 GJ m^{-2}). Net radiation is relatively low because the annual grassland has bright reflective dead vegetation in summer. In addition, the surface is very hot in summer when the grass is dead and does not transpire. Therefore the outgoing longwave radiation is substantially greater than incoming longwave radiation, causing a net loss of longwave energy (Figure 4). On an annual timescale,
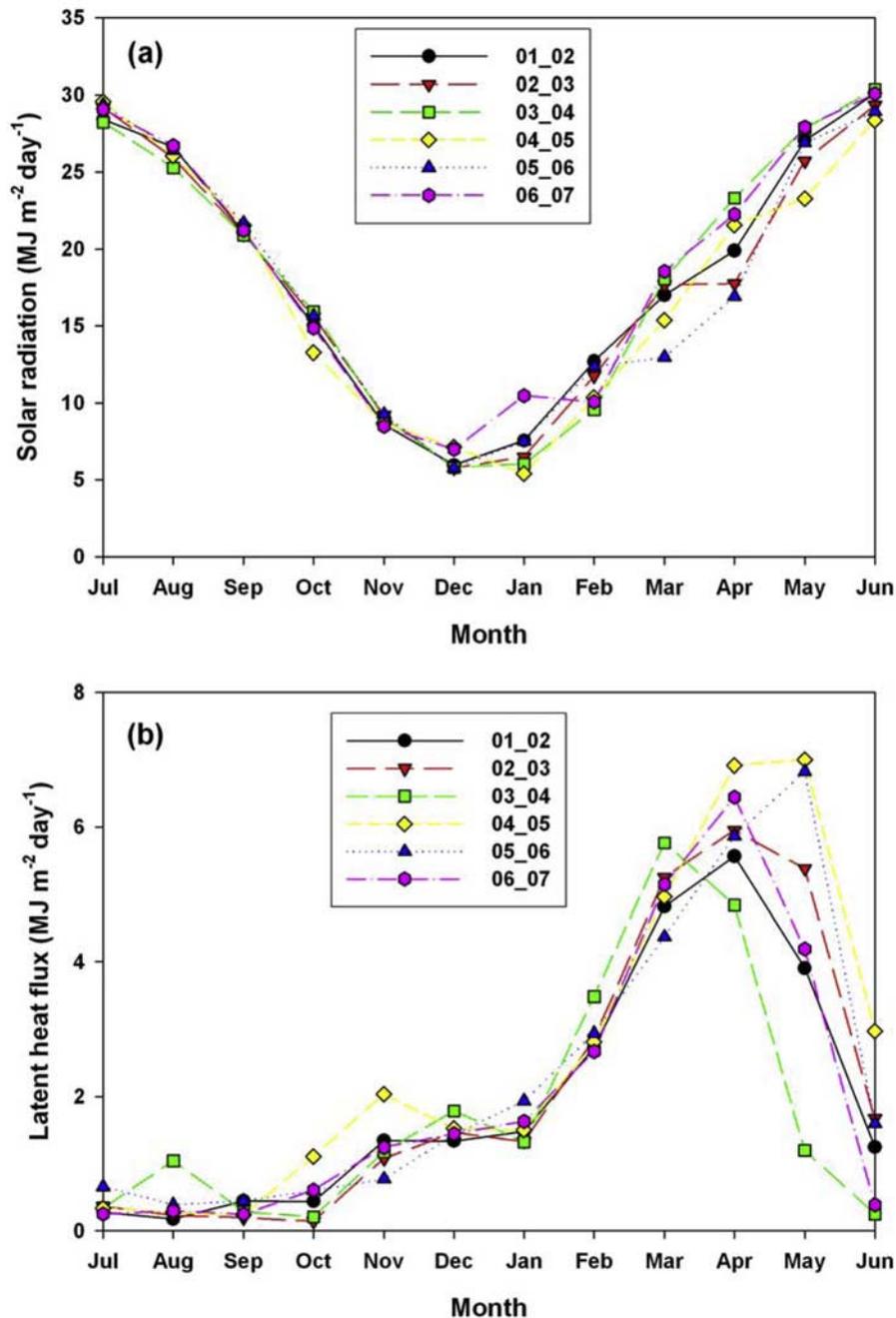
Figure 3. (a) Monthly average of daily integrated solar radiation for 6-year. (b) Monthly average of daily integrated latent heat flux for 6-year period. 01–02 indicates July 2001 to June 2002.

the main consumer of R_n in the annual grassland was sensible heat exchange, H, (67% of R_n). In comparison, λE is smaller because it only occurs in the wet seasons when the R_n is small (Figure 1). On a monthly timescale, 85% of R_n was used by λE in the growing season (January to April), whereas only 5% in the dry season (July to September). Annual sums of λE ranged from 0.66 to 0.99 GJ m^{-2} and showed a repeatable seasonal pattern from July to March during the 6-year under investigation. On the other hand, λE experienced high interannual variability between May and June, which in turn controlled the interannual

variability in annual sums of λE (Figure 3b). On an annual basis, the ratio of E to precipitation ranged from 0.39 (05–06 hydrological year) to 0.80 (06–07 hydrological year) with an average of 0.53. It is notable that the 06–07 hydrological year with the lowest rainfall (376 mm) evaporated 303 mm of water, whereas the 05–06 hydrological year had the highest rainfall (888 mm) with just 343 mm of evaporation. These data imply that the majority of rainfall either ran off or infiltrated into the unsaturated zone of the subsurface and recharged the groundwater. A large transition in λE and H occurred
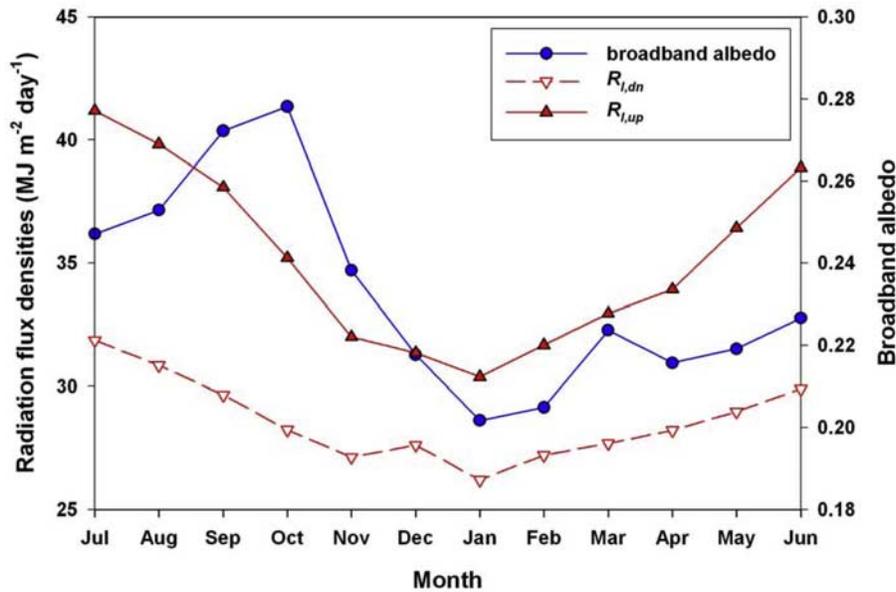
Figure 4. Mean multiyear record (03–04 to 06–07 year) of monthly average of daily integrated outgoing ($R_{l,up}$) and incoming ($R_{l,dn}$) longwave radiation, and monthly average of shortwave broadband albedo. Albedo was calculated from integrated outgoing shortwave radiation divided by integrated incoming shortwave radiation during each month.

during the senescence periods, which is in agreement with observations over a tallgrass prairie [*Ham and Knapp*, 1998] (Figure 3b). On an annual scale, *G* was negligible and nearly zero during the 6-year period.

3.4. Bulk Parameters

[22] On an annual timescale, average surface conductance, G_s, ranged between 2.8 mm s^{-1} (03–04 hydrological year) and 5.8 mm s^{-1} (04–05 hydrological year) (Table 2).

Monthly G_s in that year showed the lowest maximum G_s value (around 7 mm s^{-1}) during the 6-year and approached zero in May (Figure 1e). In contrast, the hydrological year, 04_05, showed higher maximum G_s value (around 13 mm s^{-1}) and maintained 3 mm s^{-1} by June (Figure 1e). Among the 6-year data record, only the hydrological year, 04–05, received rainfall (22 mm) in June and this rainfall extended growing season length, causing higher G_s in June than the
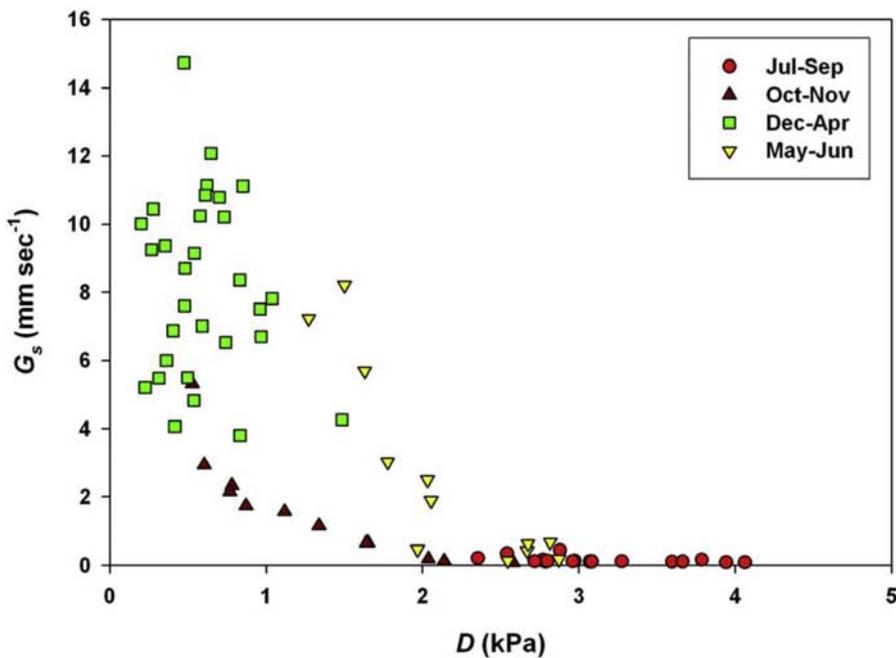

Figure 5. The relationships between monthly average vapor pressure deficit (*D*) and G_s during the 6-year period. Monthly G_s and *D* were averaged from daytime values (10:00 to 14:00).
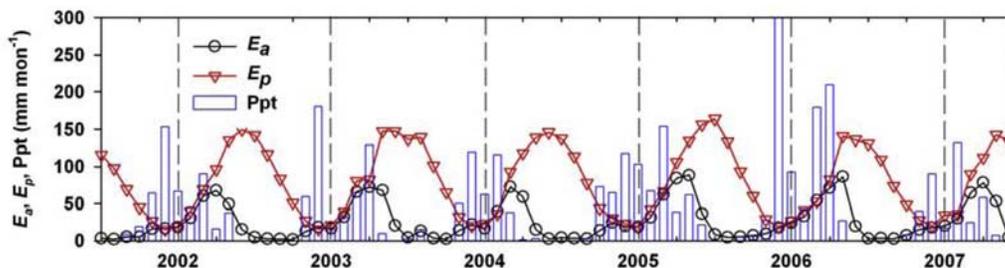
Figure 6. Time series of monthly sum of actual E (E_a), potential E (E_p) and precipitation (Ppt) from July 2001 to June 2007. Vertically dashed lines indicate January for each calendar year.

other years. Overall, G_s decreased exponentially with D (Figure 5). In the dry season (July and September), D ranged from 2.3 to 4.1 kPa and G_s was nearly zero, whereas in wet season (December to April), D was less than 1.5 kPa and G_s ranged from 4 to 15 mm sec^{-1}. G_s in two transitional periods (i.e., October to November and May to June) responded differently to similar D values ($\sim$1.5 kPa). In October to November, the grass started to germinate so that L_G is very low, less than 0.5 (Figure 1c), causing low values of G_s ($\sim$1 mm sec^{-1}) too. In contrast, G_s in May and June reached 8 mm sec^{-1} because several years maintained the high L_G with ample soil moisture in this period (e.g., 04–05 year). Consequently, G_s was more sensitive to D in May and June. The average coupling coefficient, Ω, during the 6-year period was 0.27, indicating that E is tightly controlled by its surface conductance (Table 2). On an annual timescale, the average α was 0.45, roughly half of λE_{eq}. On a monthly scale, the maximum α reached 0.97 in March of the 05–06 and 06–07 hydrological years (not shown in this paper). It indicates that maximum λE was comparable to the equilibrium λE over a wet vegetated surface.

4. Discussion
4.1. Comparison of Energy Fluxes With Other Studies

[23] The average annual R_g during the 6-year period was 6.62 GJ m^{-2}. This is higher than the tallgrass site (5.8 GJ m^{-2}) whose latitude is lower than this study site by two degrees [*Burba and Verma*, 2005] and it is among the highest values observed in North and South America [*Ohmura and Gilgen*, 1993]. The high annual energy flux of R_g is due to the clear skies in the summer. The averaged annually integrated R_n balance during the 6-year period was 2.21 GJ m^{-2}. The annual R_n is lower than the reports of 3.03 GJ m^{-2} [*Wilson and Baldocchi*, 2000] and 2.55 GJ m^{-2} [*Oliphant et al.*, 2004] over temperate deciduous forests, 2.68 GJ m^{-2} over a cypress forest in Japan [*Kosugi et al.*, 2007], 3.15 GJ m^{-2} over a woody savanna ecosystem in western US [*Baldocchi et al.*, 2004], 2.82 GJ m^{-2} over a temperate pine plantation forest in Canada [*Restrepo and Arain*, 2005], 4.09 GJ m^{-2} [*Malhi et al.*, 2002], 3.89 GJ m^{-2} [*da Rocha et al.*, 2004] and 3.82 GJ m^{-2} [*Vourlitis et al.*, 2002] over Amazonian rain forests in Brazil, 3.02 GJ m^{-2} [*Burba and Verma*, 2005] and 2.56 GJ m^{-2} [*Li et al.*, 2005] over grasslands. Only a woody savanna site after harvest in France [*Kowalski et al.*, 2003] and a Douglas fir forest in Canada [*Humphreys et al.*, 2003] experienced lower R_n values than this study, e.g.,

1.96 GJ m^{-2} and 2.13 GJ m^{-2}, respectively. It is notable that all the cited sites received less R_g than the study site, indicating that the annual grassland site received the highest energy but was least efficient in converting it to the available energy for work.

[24] Average annual E (319 mm) was comparable to many other studies in other climates and over different plant functional types. It is comparable to 320 mm [*Kljun et al.*, 2006] and 321 mm [*Lee et al.*, 1999] over Boreal mixed forests in Canada, 303 mm [*Kljun et al.*, 2006] and 320 mm [*Owen et al.*, 2007] over Boreal evergreen needleleaf forests in Canada and Finland, and 321 mm over a mixed forest in Italy [*Owen et al.*, 2007]. A few sites reported less annual E than this study site, namely 126 mm over a broadleaf deciduous forest in Finland [*Aurela et al.*, 2001], 146 mm over a deciduous needleleaf forest in Russia [*Dolman et al.*, 2004], 180 mm over an open shrubland in Israel [*Grunzweig et al.*, 2003], 220 mm over a deciduous broadleaf forest in Denmark [*Owen et al.*, 2007], and 255 mm [*Wever et al.*, 2002], 225 mm [*Amiro et al.*, 2006], 237 mm [*Kljun et al.*, 2006] over a Boreal grassland, a mixed forest, and a evergreen deciduous forest in Canada.

4.2. Constraints on E
4.2.1. Water and Energy

[25] From the standpoint of climatology, the annual grasslands of Mediterranean-type climate zones are classified as a semi-arid region, indicating that they are water-limited [*Biswell*, 1956]. On an annual timescale, the Budyko's AI (i.e., precipitation/E_p) of the study site ranged from 0.39 (03–04 year) to 0.91 (05–06 year) with the average equaling 0.59 (Table 2), confirming that this ecosystem is water-limited. Examining data on the monthly timescale, however, indicates that each year experienced both pronounced water-limited (dry season) and energy-limited (wet season) periods (Figure 6). During the dry season, E_p (i.e., water demand) was much higher than precipitation (i.e., water supply), causing AI to approach zero. Therefore actual E (E_a) in the dry season is restrained by precipitation (i.e., water-limited). During August 2003, there was an uncommon summer rainfall event, and all rainfall evaporated (Figure 6). In contrast, during the wet season, precipitation is higher than E_p, forcing AI to exceed 1 (i.e., energy-limited). Regardless of the precipitation amount, E_a was tightly controlled by E_p in the wet season. For example, there was heavy rainfall reaching 300 mm in December 2005; however, E_a was only 18 mm because E_p was just 19 mm and E_a was confined by E_p. Theoretically, E_a should be less than
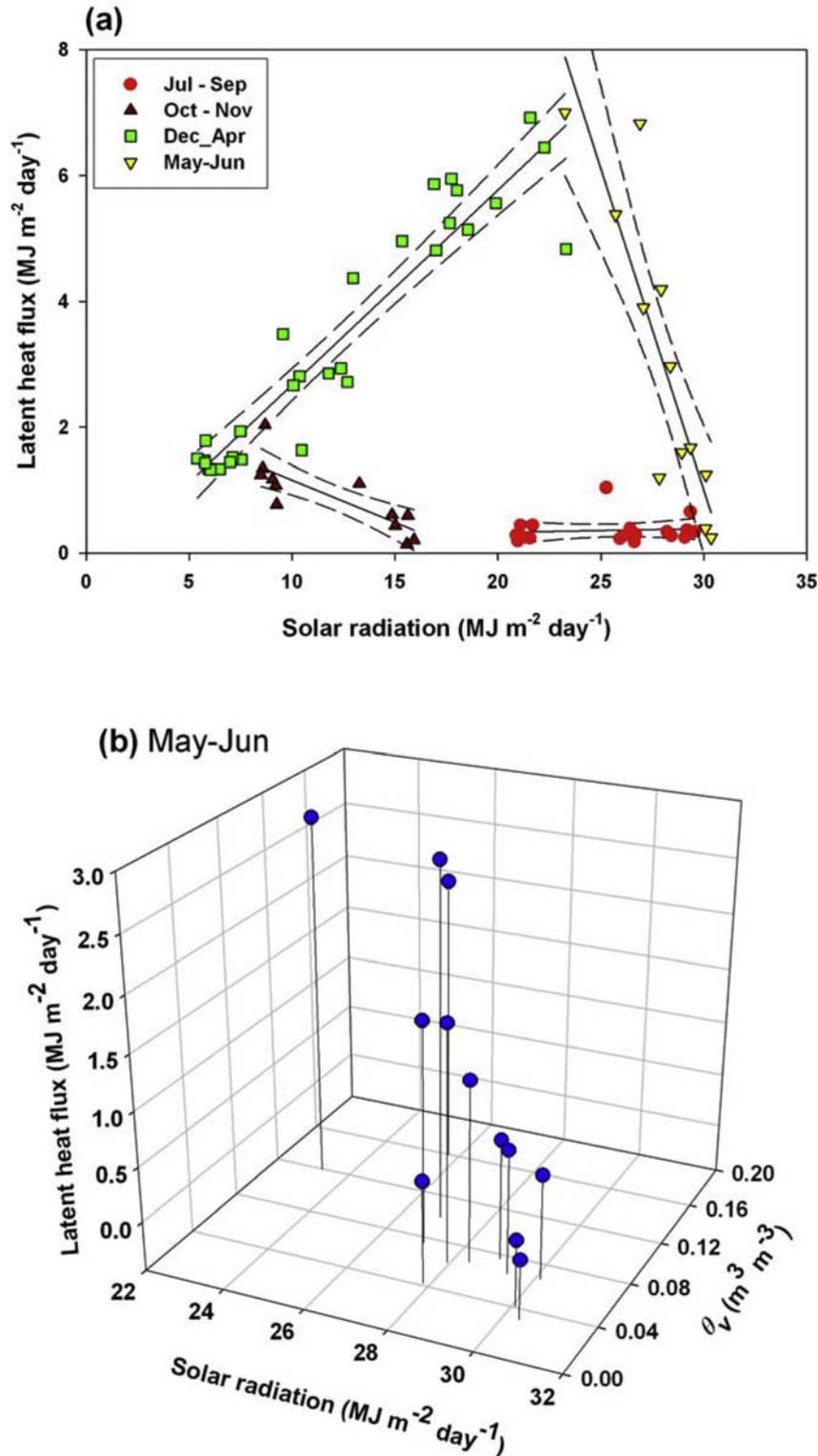
Figure 7. (a) The relationships between monthly average daily solar radiation and monthly average daily latent heat flux during the 6-year period. Dashed lines indicate 95% confidence interval of the linear regressions. (b) The relationship among monthly average daily solar radiation, monthly average volumetric soil water content at 5-cm depth (θ_v), and monthly average daily latent heat flux in May and June during the 6-year period. The points indicate the green upside-down triangles in (a).
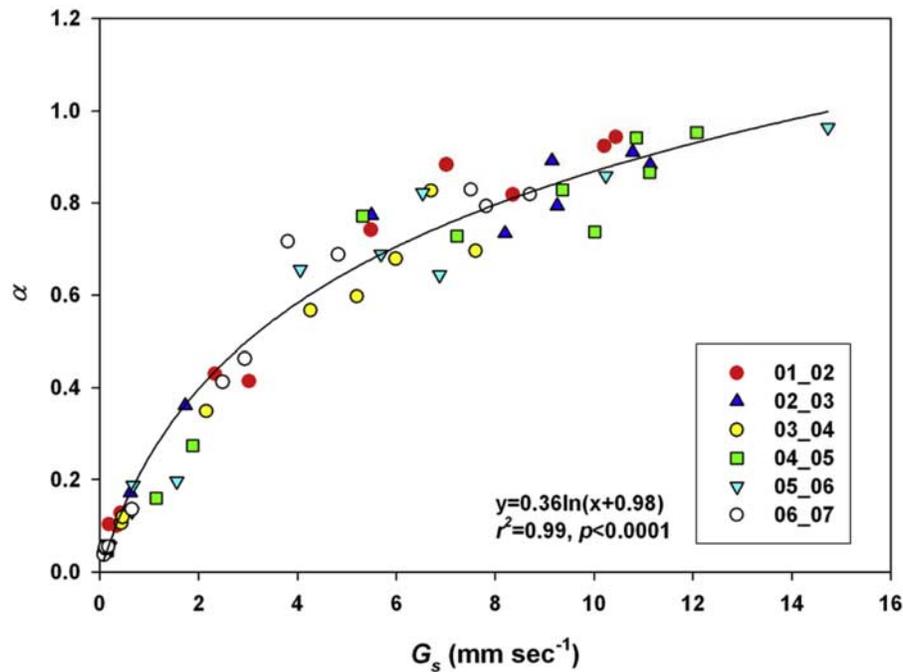
Figure 8. The relationships between monthly average bulk surface conductance (G_s) and Priestly-Taylor α coefficient. Monthly G_s and α were averaged from daytime values (10:00 to 14:00).

the minimum of E_p and precipitation [*Farquhar and Roderick*, 2007]. However, we found that E_a was higher than precipitation but lower than E_p in April or May (e.g., 2005 May). It was reported that the soil water holding capacity of the root zone is about 132 mm at this study site [*Baldocchi et al.*, 2004]. Therefore some portion of precipitation in the previous month can be stored in the soil and used in the next month, causing E_a to be higher than precipitation. Also, it should be noted that the majority of heavy precipitation (e.g., 300 mm in 2005 December) will runoff or infiltrate into groundwater considering the nearly saturated state of the subsurface and shallow rooting depth [*Aanderud et al.*, 2003; *Joffre and Rambal*, 1993]. Because Budyko's framework assumes that soil water storage and the macro-climate are at steady state and does not consider the role of vegetation, one should be cautious about interpreting Budyko's AI on short spatial and temporal scales [*Donohue et al.*, 2007].

[26] The relationship between monthly R_g and λE helps us interpret how E is modulated by the energy- and water-limited periods (Figure 7a). From July to September, λE was nearly zero and was not influenced by R_g amount because this is the dry season and there is nearly no water in the soil. In October and November, λE was negatively correlated to R_g. Precipitation in this period is critical to grass germination and growth [*Pitt and Heady*, 1978]. So E favors less R_g, more clouds and more frequent wet surface conditions. In December to April, λE scaled positively with R_g amount because there is ample water supply but paucity of available energy (i.e., energy-limited period). In May to June, λE showed remarkably negative correlation to R_g. In this water-limited period, R_g was negatively correlated to soil water content. Therefore less R_g with higher soil water

content could increase λE under higher water demand (Figure 7b). A companion study also reported that precipitation in this period was critical for extending the growing season length and increasing carbon uptake [*Ma et al.*, 2007].

4.2.2. Physiological Control via Surface Conductance

[27] Maximum daily G_s values reached 25 mm s^{-1} (not shown in the graph), which is comparable values reported for tallgrass prairie of the Great Plains; 25 mm s^{-1} [*Kim and Verma*, 1990] and 20 mm s^{-1} [*Stewart and Verma*, 1992]. It is lower than the canopy conductances for cultivated crops of the Great Plains; 29 mm s^{-1} for maize and 38 mm s^{-1} for soybean [*Suyker and Verma*, 2007]. The maximum G_s value at our study site is one of the highest values reported across diverse ecosystems [*Kelliher et al.*, 1995]. This was possible due to ample water in the growing season and high leaf nitrogen values ranging between 2 and 4% (not published), comparable to cultivated crops ranging between 1 and 5% [*Suyker and Verma*, 2007].

[28] On an annual timescale, average α was 0.45. This is lower than the report of 0.8 for a Douglas fir forest in Canada [*Humphreys et al.*, 2003] and the report of 0.72 for a temperate deciduous forest in south-eastern US [*Wilson and Baldocchi*, 2000]. It has been reported that the relation between G_s and α can represent the interactive effects of L_G, soil water status and photosynthetic capacity of any PFTs [*Baldocchi et al.*, 1997; *Baldocchi and Xu*, 2007; *deBruin*, 1983; *McNaughton and Spriggs*, 1989]. In our 6-year study, the monthly G_s scaled with α regardless of interannual and seasonal variation of precipitation and E, supporting previous studies (Figure 8). On the monthly scale, α did not exceed one, indicating E_{eq} approximately establishes the upper limit of E_a of annual grassland. Under dry canopies with well watered soil and high available energy, α of crops
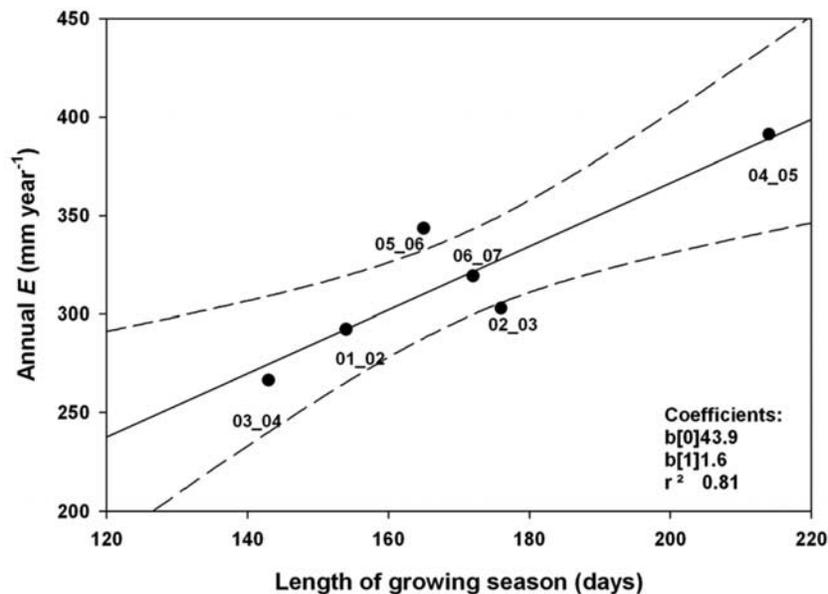
Figure 9. The relationships between growing season lengths and annual E during the 6-year period. b[0] and b[1] indicate intercept and slope, respectively. Dashed lines indicate 95% confidence interval for linear regression lines.

approaches 1.26 (i.e., E_p) [*deBruin*, 1983; *McNaughton and Spriggs*, 1989; *Priestley and Taylor*, 1972]. It is notable that the annual grassland grows in winter when R_g is the least, so it does not readily reach the E_p even though it has ample soil water. A theoretical study showed that α is insensitive to G_s when G_s exceeds about 16 mm sec^{-1} [*McNaughton and Spriggs*, 1986]. Our result showed that two variables have logarithmic relation and that α is insensitive to G_s over 12 mm sec^{-1}, supporting the theoretical study.

4.2.3. Main Determinant on Annual ET Amount: Growing Season Length

[29] Many studies have reported that longer growing seasons enhance annual carbon uptake [*Baldocchi et al.*, 2001a; *Churkina et al.*, 2005]. However, there are few studies that have investigated the effect of growing season length on annual E. In annual grassland, we observed a tight correlation between the hydrological growing season length and annual E amount (Figure 9). This ecosystem showed the distinct transition of λE in senescent period rather than the onset of a greenness period, contrary to observations in deciduous forests [*Moore et al.*, 1996; *Wilson and Baldocchi*, 2000] (Figure 3b). Therefore the timing of the onset of the senescence period is more critical to the annual E amount than the earlier onset of greenness period. It was reported that an earlier spring uses the soil water reservoir sooner and leads to summer drought in Northern Hemisphere [*Angert et al.*, 2005]. An analysis on NDVI, precipitation and surface temperature data in North American grasslands reported that lengthening growing season does not necessarily lead to more E [*Wang et al.*, 2006b]. These arguments are not applicable to the annual grassland because it has a different phenological pattern (i.e., dead in summer and active in winter). Therefore annual E scaled with the hydrological growing season length rather than the frost free growing season. These results are consistent with reports in our companion paper that annual gross primary productivity scaled with the length of the growing season at the site [*Ma et al.*, 2007].

4.3. Application of Long-Term Flux Measurements to Testing a Plant Functional Type Scheme

[30] Understanding the biophysical behavior of plant function is important for upscaling flux measurements to regional and continental level. Also, the mechanistic determination of PFTs is of particular importance for predicting the distribution of vegetation under climate change because PFTs are central to global dynamic vegetation models [*Cramer et al.*, 2001]. The PFTs are categorized using climate and vegetation information [*Bonan et al.*, 2002; *Holdridge*, 1947; *Stephenson*, 1990; *Woodward and Lomas*, 2004]. One widely used scheme for PFTs classification is the water balance approach. Traditionally, E_a was estimated as a function of air temperature [*Thornthwaite*, 1948] or as the residual between precipitation and runoff [*Eagleman*, 1976]. The long-term measurement of E_a from flux towers provides an excellent opportunity to revise and refine the water balance driven PFTs classification. *Stephenson* [1990] proposed a vegetation distribution map based on the relation between annual E_a and water deficit (i.e., E_p-precipitation) over North America. However, it evaluated E_a indirectly using the water balance method [*Eagleman*, 1976]. We compiled E_a and water deficit data across several ecosystems from the published data (Figure 10). Overall, annual E_a scaled negatively with annual water deficit, implying that biological stress (i.e., water deficit) may control annual E_a. Our 6-year direct E_a measurement over the annual grassland showed that the water deficit and E_a ranged from 100 to 650 mm and from 270 to 390 mm, respectively. We found that the ranges belong to the grassland of California in Stephenson's PFT scheme. However, annual E_a of a temperate deciduous forest in south-western US [*Wilson and Baldocchi*, 2000] ranged from 537 to 611 mm, which is
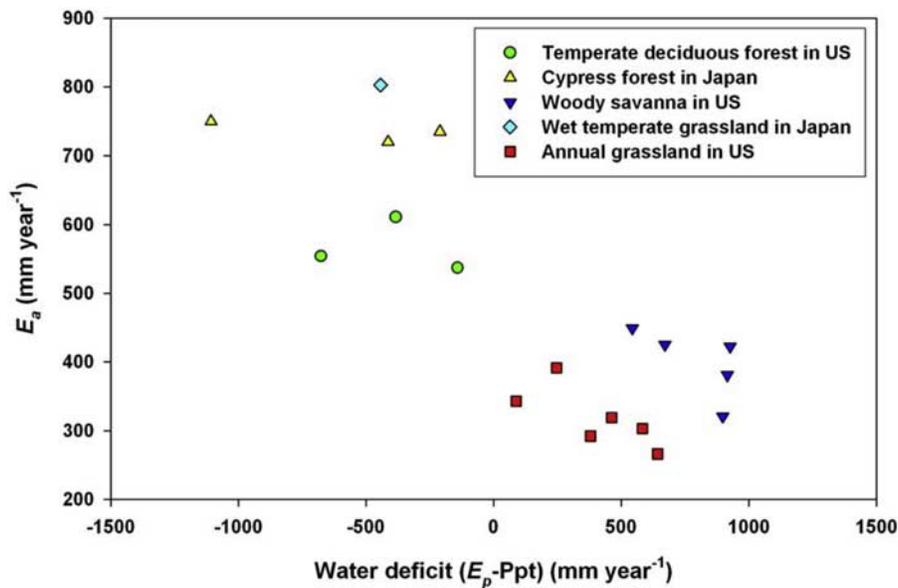
Figure 10. The relationships between annual water deficit (E_p-Ppt) and annual actual E. E_p and Ppt are potential E and precipitation. Data for a temperate deciduous forest from *Wilson and Baldocchi* [2000], a cypress forest from *Kosugi et al.* [2007], woody savanna from *Baldocchi et al.* [2004] with unpublished data, a wet temperate grassland from *Li et al.* [2005], and an annual grassland from this study. E_p was calculated from E_{eq} times 1.24.

slightly lower than Stephenson's guideline of E_a (600 to 1400 mm) for this ecosystem. Also, Stephenson's classification only covered positive water deficit, but the graph showed that there was a broad range in water deficit from −1300 mm to 1000 mm. Furthermore, ecosystems outside US showed different E_a and water deficit compared to Stephenson's diagram. For example, E_a of a cypress forest in Japan ranged from 720 to 750 mm, which is higher than Stephenson's guideline (240 to 600 mm) (Figure 10) [*Kosugi et al.*, 2007]. For a wet temperate grassland in Japan, annual E_a reached 800 mm, which is much higher than the annual grassland of this study and cannot be classified within Stephenson's framework. It should be noted that Stephenson's classification is for North America, so it may not be applicable outside North America. It is expected that the growing FLUXNET database across diverse ecosystems can contribute to revising and refining the PFTs schemes, and it will clearly help to scale-up flux data into regional and continental scales.

5. Summary and Conclusions

[31] In this study, we reported on the interannual variability of E and energy fluxes over an annual grassland growing in the Mediterranean-type climate in California using a 6-year flux measurement. The Mediterranean climate system of the study site has two distinct seasons. One is a wet period during winter with ample water and low solar radiation. The other is a dry period in summer with scarce soil water and high levels of solar radiation. Consequently, ecosystem E experiences both water-limited and energy-limited periods during the year. In the energy-limited period, the majority of E scaled positively with R_g and was confined by E_p. In the water-limited period, however, most

E was down-regulated by stomatal closure and scaled negatively with R_g. In general, high rainfall in wet season did not lead to high E because of the marginal available energy. Therefore the annual E amount of this ecosystem was not sensitive to annual precipitation amount. Rather, the lifespan of the annual grassland that was coincident with the timing of rainfall was critical in determining the hydrological growing season length and the amount of annual E. Rainfall in May and June was especially critical in extending the growing season and E. We expect that the cloud cover and precipitation regime in May and June will play a key role in modulating annual E amount in this ecosystem in future years. G_s scaled tightly with α regardless of interannual and seasonal variability of precipitation, E, and R_g, implying that this relationship may be used to discern PFTs. Additionally, we showed that long-term flux measurement can be used to test classification of PFTs, which is critical to upscale flux measurements into regional and continental scales.

References

Aanderud, Z. T., C. S. Bledsoe, and J. H. Richards (2003), Contribution of relative growth rate to root foraging by annual and perennial grasses from California oak woodlands, *Oecologia*, *136*(3), 424–430.

Amiro, B. D., et al. (2006), Carbon, energy and water fluxes at mature and disturbed forest sites, Saskatchewan, Canada, *Agric. For. Meteorol.*, *136*(3–4), 237–251.

Angert, A., S. Biraud, C. Bonfils, C. C. Henning, W. Buermann, J. Pinzon, C. J. Tucker, and I. Fung (2005), Drier summers cancel out the CO_2 uptake enhancement induced by warmer springs, *Proc. Natl. Acad. Sci. U.S.A.*, *102*(31), 10,823–10,827.

Arain, M. A., T. A. Black, A. G. Barr, P. G. Jarvis, J. M. Massheder, D. L. Verseghy, and Z. Nesic (2002), Effects of seasonal and inter-annual climate variability on net ecosystem productivity of boreal deciduous and conifer forests, *Can. J. For. Res.*, *32*(5), 878–891.

Arain, M. A., T. A. Black, A. G. Barr, T. J. Griffis, K. Morgenstern, and Z. Nesic (2003), Year-round observations of the energy and water vapour fluxes above a boreal black spruce forest, *Hydrol. Processes*, *17*(18), 3581–3600.

Aurela, M., J. P. Tuovinen, and T. Laurila (2001), Net CO_2 exchange of a subarctic mountain birch ecosystem, *Theor. Appl. Climatol.*, *70*(1–4), 135–148.

Baldocchi, D., and T. Meyers (1998), On using eco-physiological, micro-meteorological and biogeochemical theory to evaluate carbon dioxide, water vapor and trace gas fluxes over vegetation: A perspective, *Agric. For. Meteorol.*, *90*(1–2), 1–25.

Baldocchi, D. D., and L. K. Xu (2007), What limits evaporation from Mediterranean oak woodlands-The supply of moisture in the soil, physiological control by plants or the demand by the atmosphere, *Adv. Water Resour.*, *30*, 2113–2122.

Baldocchi, D. D., C. A. Vogel, and B. Hall (1997), Seasonal variation of energy and water vapor exchange rates above and below a boreal jack pine forest canopy, *J. Geophys. Res.*, *102*(D24), 28,939–28,951.

Baldocchi, D., et al. (2001a), FLUXNET: A new tool to study the temporal and spatial variability of ecosystem-scale carbon dioxide, water vapor, and energy flux densities, *Bull. Am. Meteorol. Soc.*, *82*(11), 2415–2434.

Baldocchi, D., E. Falge, and K. Wilson (2001b), A spectral analysis of biosphere-atmosphere trace gas flux densities and meteorological variables across hour to multi-year time scales, *Agric. For. Meteorol.*, *107*(1), 1–27.

Baldocchi, D. D., L. K. Xu, and N. Kiang (2004), How plant functional-type, weather, seasonal drought, and soil physical properties alter water and energy fluxes of an oak-grass savanna and an annual grassland, *Agric. For. Meteorol.*, *123*(1–2), 13–39.

Barford, C. C., S. C. Wofsy, M. L. Goulden, J. W. Munger, E. H. Pyle, S. P. Urbanski, L. Hutyra, S. R. Saleska, D. Fitzjarrald, and K. Moore (2001), Factors controlling long- and short-term sequestration of atmospheric CO_2 in a mid-latitude forest, *Science*, *294*(5547), 1688–1691.

Barr, A. G., T. A. Black, E. H. Hogg, T. J. Griffis, K. Morgenstern, N. Kljun, A. Theede, and Z. Nesic (2007), Climatic controls on the carbon and water balances of a boreal aspen forest, 1994–2003, *Global Change Biol.*, *13*(3), 561–576.

Beringer, J., L. B. Hutley, N. J. Tapper, and L. A. Cernusak (2007), Savanna fires and their impact on net ecosystem productivity in North Australia, *Global Change Biol.*, *13*(5), 990–1004.

Biswell, H. H. (1956), Ecology of California grasslands, *J. Range Manage.*, *9*(1), 19–24.

Bonan, G. B., S. Levis, L. Kergoat, and K. W. Oleson (2002), Landscapes as patches of plant functional types: An integrating concept for climate and ecosystem models, *Global Biogeochem. Cycles*, *16*(2), 1021, doi:10.1029/2000GB001360.

Bosch, J. M., and J. D. Hewlett (1982), A review of catchment experiments to determine the effect of vegetation changes on water yield and evapotranspiration, *J. Hydrol.*, *55*(1–4), 3–23.

Bremer, D. J., L. M. Auen, J. M. Ham, and C. E. Owensby (2001), Evapotranspiration in a prairie ecosystem: Effects of grazing by cattle, *Agron. J.*, *93*(2), 338–348.

Brubaker, K. L., and D. Entekhabi (1996), Analysis of feedback mechanisms in land-atmosphere interaction, *Water Resour. Res.*, *32*(5), 1343–1357.

Brutsaert, W. (2006), Cations of increasing land surface evaporation during the second half of the 20th century, *Geophys. Res. Lett.*, *33*(20), L20403, doi:10.1029/2006GL027532.

Brutsaert, W., and M. B. Parlange (1998), Hydrologic cycle explains the evaporation paradox, *Nature*, *396*(6706), 30.

Budyko, M. I. (1974), *Climate and Life*, Academic Press, New York, NY.

Burba, G. G., and S. B. Verma (2001), Prairie growth, PAR albedo and seasonal distribution of energy fluxes, *Agric. For. Meteorol.*, *107*(3), 227–240.

Burba, G. G., and S. B. Verma (2005), Seasonal and interannual variability in evapotranspiration of native tallgrass prairie and cultivated wheat ecosystems, *Agric. For. Meteorol.*, *135*(1–4), 190–201.

Carrara, A., A. S. Kowalski, J. Neirynck, I. A. Janssens, J. C. Yuste, and R. Ceulemans (2003), Net ecosystem CO_2 exchange of mixed forest in Belgium over 5 years, *Agric. For. Meteorol.*, *119*(3–4), 209–227.

Churkina, G., D. Schimel, B. H. Braswell, and X. M. Xiao (2005), Spatial analysis of growing season length control over net ecosystem exchange, *Global Change Biol.*, *11*(10), 1777–1787.

Cramer, W., et al. (2001), Global response of terrestrial ecosystem structure and function to CO_2 and climate change: Results from six dynamic global vegetation models, *Global Change Biol.*, *7*(4), 357–373.

da Rocha, H. R., M. L. Goulden, S. D. Miller, M. C. Menton, L. Pinto, H. C. de Freitas, and A. Figueira (2004), Seasonality of water and heat fluxes over a tropical forest in eastern Amazonia, *Ecol. Appl.*, *14*(4), S22–S32.

Dai, A., I. Y. Fung, and A. D. DelGenio (1997), Surface observed global land precipitation variations during 1900–88, *J. Clim.*, *10*(11), 2943–2962.

deBruin, H. A. R. (1983), A model for the Priestley-Taylor parameter-alpha, *J. Clim. Appl. Meteorol.*, *22*(4), 572–578.

Dolman, A. J., T. C. Maximov, E. J. Moors, A. P. Maximov, J. A. Elbers, A. V. Kononov, M. J. Waterloo, and M. K. van der Molen (2004), Net ecosystem exchange of carbon dioxide and water of far eastern Siberian Larch (Larix cajanderii) on permafrost, *Biogeosciences*, *1*(2), 133–146.

Donohue, R. J., M. L. Roderick, and T. R. McVicar (2007), On the importance of including vegetation dynamics in Budyko's hydrological model, *Hydrol. Earth Syst. Sci.*, *11*(2), 983–995.

Dunn, A. L., C. C. Barford, S. C. Wofsy, M. L. Goulden, and B. C. Daube (2007), A long-term record of carbon exchange in a boreal black spruce forest: Means, responses to interannual variability, and decadal trends, *Global Change Biol.*, *13*(3), 577–590.

Eagleman, J. R. (1976), *The Visualization of Climate*, Lexington Books, Lexington, Mass.

Efron, B., and R. J. Tibshirani (1993), *An Introduction to the Bootstrap*, Chapman & Hall, New York.

Falge, E., et al. (2001), Gap filling strategies for long term energy flux data sets, *Agric. For. Meteorol.*, *107*(1), 71–77.

Farquhar, G. D., and M. L. Roderick (2007), Worldwide changes in evaporative demand, Proceedings of the Pontifical Academy of Sciences, in press.

Garratt, J. R., and B. B. Hicks (1973), Momentum, heat and water-vapor transfer to and from natural and artificial surfaces, *Q. J. R. Meteorol. Soc.*, *99*(422), 680–687.

Gedney, N., P. M. Cox, R. A. Betts, O. Boucher, C. Huntingford, and P. A. Stott (2006), Detection of a direct carbon dioxide effect in continental river runoff records, *Nature*, *439*(7078), 835–838.

Gilmanov, T. G., T. J. Svejcar, D. A. Johnson, R. E. Angell, N. Z. Saliendra, and B. K. Wylie (2006), Long-term dynamics of production, respiration, and net CO_2 exchange in two sagebrush-steppe ecosystems, *Rangeland Ecol. Manage.*, *59*(6), 585–599.

Golubev, V. S., J. H. Lawrimore, P. Y. Groisman, N. A. Speranskaya, S. A. Zhuravin, M. J. Menne, T. C. Peterson, and R. W. Malone (2001), Evaporation changes over the contiguous United States and the former USSR: A reassessment, *Geophys. Res. Lett.*, *28*(13), 2665–2668.

Grace, J., J. Lloyd, A. C. Miranda, H. Miranda, and J. H. C. Gash (1998), Fluxes of carbon dioxide and water vapour over a C-4 pasture in south-western Amazonia (Brazil), *Aust. J. Plant Physiol.*, *25*(5), 519–530.

Groisman, P. Y., R. W. Knight, T. R. Karl, D. R. Easterling, B. M. Sun, and J. H. Lawrimore (2004), Contemporary changes of the hydrological cycle over the contiguous United States: Trends derived from in situ observations, *J. Hydrometeorol.*, *5*(1), 64–85.

Grunwald, T., and C. Bernhofer (2007), A decade of carbon, water and energy flux measurements of an old spruce forest at the Anchor Station Tharandt, *Tellus, Ser. B*, *59*(3), 387–396.

Grunzweig, J. M., T. Lin, E. Rotenberg, A. Schwartz, and D. Yakir (2003), Carbon sequestration in arid-land forest, *Global Change Biol.*, *9*(5), 791–799.

Hagen, S. C., B. H. Braswell, E. Linder, S. Frolking, A. D. Richardson, and D. Y. Hollinger (2006), Statistical uncertainty of eddy flux-based estimates of gross ecosystem carbon exchange at Howland Forest, Maine, *J. Geophys. Res.*, *111*, D08503, doi:10.1029/2005JD006154.

Ham, J. M., and A. K. Knapp (1998), Fluxes of CO_2 water vapor, and energy from a prairie ecosystem during the seasonal transition from carbon sink to carbon source, *Agric. For. Meteorol.*, *89*(1), 1–14.

Hanson, P. J., et al. (2004), Oak forest carbon and water simulations: Model intercomparisons and evaluations against independent data, *Ecol. Monogr.*, *74*(3), 443–489.

Haszpra, L., Z. Barcza, K. J. Davis, and K. Tarczay (2005), Long-term tall tower carbon dioxide flux monitoring over an area of mixed vegetation, *Agric. For. Meteorol.*, *132*(1–2), 58–77.

Heusinkveld, B. G., A. F. G. Jacobs, A. A. M. Holtslag, and S. M. Berkowicz (2004), Surface energy balance closure in an arid region: Role of soil heat flux, *Agric. For. Meteorol.*, *122*(1–2), 21–37.

Holdridge, L. R. (1947), Determination of world plant formations from simple climatic data, *Science*, *105*(2727), 367–368.

Hollinger, D. Y., et al. (2004), Spatial and temporal variability in forest-atmosphere CO₂ exchange, *Global Change Biol.*, *10*(10), 1689–1706.

Houghton, J. T., Y. Ding, D. C. Griggs, M. Noguer, P. J. van der Linden, X. Dai, K. Maskell, and C. A. Johnson (2001), *Climate Change 2001: The Scientific Basis*, Cambridge University Press, Cambridge, UK.

Hulme, M., T. J. Osborn, and T. C. Johns (1998), Precipitation sensitivity to global warming: Comparison of observations with HadCM2 simulations, *Geophys. Res. Lett.*, *25*(17), 3379–3382.

Humphreys, E. R., T. A. Black, G. J. Ethier, G. B. Drewitt, D. L. Spittlehouse, E. M. Jork, Z. Nesic, and N. J. Livingston (2003), Annual and seasonal variability of sensible and latent heat fluxes above a coastal Douglas-fir forest, British Columbia, Canada, *Agric. For. Meteorol.*, *115*(1–2), 109–125.

Hunt, J. E., F. M. Kelliher, T. M. McSeveny, and J. N. Byers (2002), Evaporation and carbon dioxide exchange between the atmosphere and a tussock grassland during a summer drought, *Agric. For. Meteorol.*, *111*(1), 65–82.

Huntington, T. G. (2006), Evidence for intensification of the global water cycle: Review and synthesis, *J. Hydrol.*, *319*(1–4), 83–95.

Hutyra, L., J. W. Munger, S. R. Saleska, E. Gottlieb, B. C. Daube, A. L. Dunn, D. F. Amaral, P. B. de Camargo, and S. C. Wofsy (2007), Seasonal controls on the exchange of carbon and water in an Amazonian rain forest, *J. Geophys. Res.*, *112*, G03008, doi:10.1029/2006JG000365.

Jacobs, A. F. G., B. G. Heusinkveld, and A. A. M. Holtslag (2007), Seasonal and interannual variability of carbon dioxide and water balances of a grassland, *Clim. Change*, *82*(1–2), 163–177.

Jaeger, L., and A. Kessler (1997), Twenty years of heat and water balance climatology at the Hartheim pine forest, Germany, *Agric. For. Meteorol.*, *84*(1–2), 25–36.

Jarvis, P. G., and K. G. McNaughton (1986), Stomal control of transpiration: scaling up from leaf to region, *Adv. Ecol. Res.*, *15*, 1–49.

Joffre, R., and S. Rambal (1993), How tree cover influences the water-balance of Mediterranean Rangelands, *Ecology*, *74*(2), 570–582.

Jones, P. D., and A. Moberg (2003), Hemispheric and large-scale surface air temperature variations: An extensive revision and an update to 2001, *J. Clim.*, *16*(2), 206–223.

Keeling, C. D., J. F. S. Chin, and T. P. Whorf (1996), Increased activity of northern vegetation inferred from atmospheric CO2 measurements, *Nature*, *382*(6587), 146–149.

Kelliher, F. M., R. Leuning, M. R. Raupach, and E.-D. Schulze (1995), Maximum conductances for evaporation from global vegetation types, *Agric. For. Meteorol.*, *73*, 1–16.

Kim, J., and S. B. Verma (1990), Components of surface-energy balance in a temperate grassland ecosystem, *Boundary Layer Meteorol.*, *51*(4), 401–417.

Kim, J., Q. Guo, D. D. Baldocchi, M. Leclerc, L. Xu, and H. P. Schmid (2006), Upscaling fluxes from tower to landscape: Overlaying flux footprints on high-resolution (IKONOS) images of vegetation cover, *Agric. For. Meteorol.*, *136*(3–4), 132–146.

Kljun, N., T. A. Black, T. J. Griffis, A. G. Barr, D. Gaumont-Guay, K. Morgenstern, J. H. McCaughey, and Z. Nesic (2006), Response of net ecosystem productivity of three boreal forest stands to drought, *Ecosystems*, *9*(7), 1128–1144.

Knapp, A. K., and M. D. Smith (2001), Variation among biomes in temporal dynamics of aboveground primary production, *Science*, *291*(5503), 481–484.

Knapp, A. K., P. A. Fay, J. M. Blair, S. L. Collins, M. D. Smith, J. D. Carlisle, C. W. Harper, B. T. Danner, M. S. Lett, and J. K. McCarron (2002), Rainfall variability, carbon cycling, and plant species diversity in a mesic grassland, *Science*, *298*(5601), 2202–2205.

Kosugi, Y., S. Takanashi, H. Tanaka, S. Ohkubo, M. Tani, M. Yano, and T. Katayama (2007), Evapotranspiration over a Japanese cypress forest. I. Eddy covariance fluxes and surface conductance characteristics for 3 years, *J. Hydrol.*, *337*(3–4), 269–283.

Kowalski, S., M. Sartore, R. Burlett, P. Berbigier, and D. Loustau (2003), The annual carbon budget of a French pine forest (Pinus pinaster) following harvest, *Global Change Biol.*, *9*(7), 1051–1065.

Labat, D., Y. Godderis, J. L. Probst, and J. L. Guyot (2004), Evidence for global runoff increase related to climate warming, *Adv. Water Resour.*, *27*(6), 631–642.

Lafleur, P. M., R. A. Hember, S. W. Admiral, and N. T. Roulet (2005), Annual and seasonal variability in evapotranspiration and water table at a shrub-covered bog in southern Ontario, Canada, *Hydrol. Processes*, *19*(18), 3533–3550.

Lee, X. H., J. D. Fuentes, R. M. Staebler, and H. H. Neumann (1999), Long-term observation of the atmospheric exchange of CO2 with a temperate deciduous forest in southern Ontario, Canada, *J. Geophys. Res.*, *104*(D13), 15,975–15,984.

Lettenmaier, D. P., and J. S. Famiglietti (2006), Water from on high, *Nature*, *444*(7119), 562–563.

Lewis, D., M. J. Singer, R. A. Dahlgren, and K. W. Tate (2000), Hydrology in a California oak woodland watershed: A 17-year study, *J. Hydrol.*, *240*(1–2), 106–117.

Li, S. G., C. T. Lai, G. Lee, S. Shimoda, T. Yokoyama, A. Higuchi, and T. Oikawa (2005), Evapotranspiration from a wet temperate grassland and its sensitivity to microenvironmental variables, *Hydrol. Processes*, *19*(2), 517–532.

Liepert, B. G., J. Feichter, U. Lohmann, and E. Roeckner (2004), Can aerosols spin down the water cycle in a warmer and moister world?, *Geophys. Res. Lett.*, *31*(6), L06207, doi:10.1029/2003GL019060.

Liu, B. H., M. Xu, M. Henderson, and W. G. Gong (2004), A spatial analysis of pan evaporation trends in China, 1955–2000, *J. Geophys. Res.*, *109*(D15), D15102, doi:10.1029/2004JD004511.

Luo, H. Y., W. C. Oechel, S. J. Hastings, R. Zulueta, Y. H. Qian, and H. Kwon (2007), Mature semiarid chaparral ecosystems can be a significant sink for atmospheric carbon dioxide, *Global Change Biol.*, *13*(2), 386–396.

Ma, S., D. D. Baldocchi, L. Xu, and T. Hehn (2007), Inter-annual variability in carbon dioxide exchange of an oak/grass savanna and open grassland in California, *Agric. For. Meteorol.*, *147*(3–4), 157–171.

Malhi, Y., E. Pegoraro, A. D. Nobre, M. G. P. Pereira, J. Grace, A. D. Culf, and R. Clement (2002), Energy and water dynamics of a central Amazonian rain forest, *J. Geophys. Res.*, *107*(D20), 8061, doi:10.1029/2001JD000623.

Marc, V., and M. Robinson (2007), The long-term water balance (1972–2004) of upland forestry and grassland at Plynlimon, mid-Wales, *Hydrol. Earth Syst. Sci.*, *11*(1), 44–60.

McNaughton, K. G., and T. W. Spriggs (1986), A mixed-layer model for regional evaporation, *Boundary Layer Meteorol.*, *34*, 243–262.

McNaughton, K. G., and T. W. Spriggs (1989), An evaluation of the Priestley and Taylor equation and the complementary relationship using results from a mixed-layer model of the convective boundary layer, paper presented at Estimation of Areal Evapotranspiration, IAHS Publication Vancouver, Canada.

Meyers, T. P. (2001), A comparison of summertime water and CO2 fluxes over rangeland for well watered and drought conditions, *Agric. For. Meteorol.*, *106*(3), 205–214.

Meyers, T. P., and S. E. Hollinger (2004), An assessment of storage terms in the surface energy balance of maize and soybean, *Agric. For. Meteorol.*, *125*(1–2), 105–115.

Monson, R. K., J. P. Sparks, T. N. Rosenstiel, L. E. Scott-Denton, T. E. Huxman, P. C. Harley, A. A. Turnipseed, S. P. Burns, B. Backlund, and J. Hu (2005), Climatic influences on net ecosystem CO₂ exchange during the transition from wintertime carbon source to springtime carbon sink in a high-elevation, subalpine forest, *Oecologia*, *146*(1), 130–147.

Monteith, J. L. (1965), Evaporation and the environment, *Symposium of the Society of Exploratory Biology*, *19*, 205–234.

Monteith, J. L., and M. H. Unsworth (1990), *Principles of Environmental Physics*, 2nd ed., Butterworth-Heinemann Ltd, London.

Moore, K. E., D. R. Fitzjarrald, R. K. Sakai, M. L. Goulden, J. W. Munger, and S. C. Wofsy (1996), Seasonal variation in radiative and turbulent exchange at a deciduous forest in central Massachusetts, *J. Appl. Meteorol.*, *35*(1), 122–134.

Morton, F. I. (1978), Estimating evapotranspiration from potential evaporation: Practicality of an iconoclastic approach, *J. Hydrol.*, *38*, 1–32.

Novick, K. A., P. C. Stoy, G. G. Katul, D. S. Ellsworth, M. B. S. Siqueira, J. Juang, and R. Oren (2004), Carbon dioxide and water vapor exchange in a warm temperate grassland, *Oecologia*, *138*(2), 259–274.

Ohmura, A., and H. Gilgen (1993), *Re-Evaluation of the Global Energy Balance*, pp. 93–110, IUGG and AGU, Washington, D.C.

Ohmura, A., and M. Wild (2002), Is the hydrological cycle accelerating?, *Science*, *298*(5597), 1345–1346.

Oliphant, A. J., C. S. B. Grimmond, H. N. Zutter, H. P. Schmid, H. B. Su, S. L. Scott, B. Offerle, J. C. Randolph, and J. Ehman (2004), Heat storage and energy balance fluxes for a temperate deciduous forest, *Agric. For. Meteorol.*, *126*(3–4), 185–201.

Owen, K. E., et al. (2007), Linking flux network measurements to continental scale simulations: Ecosystem carbon dioxide exchange capacity under non-water-stressed conditions, *Global Change Biol.*, *13*(4), 734–760.

Parton, W. J., D. S. Ojima, and D. S. Schimel (1994), Environmental-change in grasslands — Assessment using models, *Clim. Change*, *28*(1–2), 111–141.

Peterson, T. C., V. S. Golubev, and P. Y. Groisman (1995), Evaporation losing its strength, *Nature*, *377*(6551), 687–688.

Pitt, M. D., and H. F. Heady (1978), Responses of annual vegetation to temperature and rainfall patterns in northern California, *Ecology*, *59*(2), 336–350.

Priestley, C. H. B., and R. J. Taylor (1972), On the assessment of surface heat flux and evaporation using large-scale parameters, *Mon. Weather Rev.*, *100*(2), 81–92.

Ramanathan, V., P. J. Crutzen, J. T. Kiehl, and D. Rosenfeld (2001), Aerosols, climate, and the hydrological cycle, *Science*, *294*(5549), 2119–2124.

Raupach, M. R. (1995), Vegetation-atmosphere interaction and surface conductance at leaf, canopy and regional scales, *Agric. For. Meteorol.*, *73*, 151–179.

Raupach, M. R. (1998), Influences of local feedbacks on land-air exchanges of energy and carbon, *Global Change Biol.*, *4*(5), 477–494.

Restrepo, N. C., and M. A. Arain (2005), Energy and water exchanges from a temperate pine plantation forest, *Hydrol. Processes*, *19*(1), 27–49.

Roderick, M. L., and G. D. Farquhar (2002a), The cause of decreased pan evaporation over the past 50 years, *Science*, *298*(5597), 1410–1411.

Roderick, M. L., and G. D. Farquhar (2002b), The cause of decreased pan evaporation over the past 50 years, *Science*, *298*, 1410–1411.

Roulet, N. T., P. M. Lafleur, P. J. H. Richard, T. R. Moore, E. R. Humphreys, and J. Bubier (2007), Contemporary carbon balance and late Holocene carbon accumulation in a northern peatland, *Global Change Biol.*, *13*(2), 397–411.

Rouse, W. R., C. M. Oswald, J. Binyamin, P. D. Blanken, W. M. Schertzer, and C. Spence (2003), Interannual and seasonal variability of the surface energy balance and temperature of central Great Slave Lake, *J. Hydrometeorol.*, *4*(4), 720–730.

Saigusa, N., T. Oikawa, and S. Liu (1998), Seasonal variations of the exchange of CO_2 and H_2O between a grassland and the atmosphere: An experimental study, *Agric. For. Meteorol.*, *89*(2), 131–139.

Song, J. (1999), Phenological influences on the albedo of prairie grassland and crop fields, *Int. J. Biometeorol.*, *42*(3), 153–157.

Stephenson, N. L. (1990), Climatic control of vegetation distribution — The role of the water-balance, *Am. Nat.*, *135*(5), 649–670.

Stewart, J. B., and S. B. Verma (1992), Comparison of surface fluxes and conductances at 2 contrasting sites within the FIFE area, *J. Geophys. Res.*, *97*(D17), 18,623–18,628.

Suyker, A. E., and S. B. Verma (2007), Interannual water vapor and energy exchange in an irrigated maize-based agroecosystem, *Agric. For. Meteorol.*, *148*, 417–427.

Thom, A. S. (1972), Momentum, mass and heat exchange of vegetation, *Q. J. R. Meteorol. Soc.*, *98*, 124–134.

Thornthwaite, C. W. (1948), An approach toward a rational classification of climate, *Geogr. Rev.*, *38*(1), 55–94.

Valentini, R., J. A. Gamon, and C. B. Field (1995), Ecosystem gas-exchange in a California Grassland — Seasonal patterns and implications for scaling, *Ecology*, *76*(6), 1940–1952.

Verma, S. (1989), Aerodynamic resistances to transfers of heat, mass and momentum, paper presented at Estimation of Areal Evapotranspiration, IAHS Publication Vancouver, Canada.

Verma, S. B., J. Kim, and R. J. Clement (1989), Carbon-dioxide, water-vapor and sensible heat fluxes over a tallgrass prairie, *Boundary Layer Meteorol.*, *46*(1–2), 53–67.

Verma, S. B., J. Kim, and R. J. Clement (1992), Momentum, water-vapor, and carbon-dioxide exchange at a centrally located Prairie site During FIFE, *J. Geophys. Res.*, *97*(D17), 18,629–18,639.

Vourlitis, G. L., N. Priante, M. M. S. Hayashi, J. D. Nogueira, F. T. Caseiro, and J. H. Campelo (2002), Seasonal variations in the evapotranspiration of a transitional tropical forest of Mato Grosso, Brazil, *Water Resour. Res.*, *38*(6), 1094, doi:10.1029/2000WR000122.

Wang, A., D. T. Price, and V. Arora (2006a), Estimating changes in global vegetation cover (1850–2100) for use in climate models, *Global Biogeochem. Cycles*, *20*, GB3028, doi:10.1029/2005GB002514.

Wang, W. L., B. T. Anderson, N. Phillips, R. K. Kaufmann, C. Potter, and R. B. Myneni (2006b), Feedbacks of vegetation on summertime climate variability over the North American grasslands. Part I: Statistical analysis, *Earth Interactions*, *10*(1), 27.

Wetherald, R. T., and S. Manabe (2002), Simulation of hydrologic changes associated with global warming, *J. Geophys. Res.*, *107*(D19), 4379, doi:10.1029/2001JD001195.

Wever, L. A., L. B. Flanagan, and P. J. Carlson (2002), Seasonal and interannual variation in evapotranspiration, energy balance and surface conductance in a northern temperate grassland, *Agric. For. Meteorol.*, *112*(1), 31–49.

Wild, M., A. Ohmura, H. Gilgen, and D. Rosenfeld (2004), On the consistency of trends in radiation and temperature records and implications for the global hydrological cycle, *Geophys. Res. Lett.*, *31*(11), L11201, doi:10.1029/2003GL019188.

Wilson, K. B., and D. D. Baldocchi (2000), Seasonal and interannual variability of energy fluxes over a broadleaved temperate deciduous forest in North America, *Agric. For. Meteorol.*, *100*(1), 1–18.

Wilson, K. B., and D. D. Baldocchi (2001), Comparing independent estimates of carbon dioxide exchange over 5 years at a deciduous forest in the southeastern United States, *J. Geophys. Res.*, *106*(D24), 34,167–34,178.

Wilson, K., et al. (2002), Energy balance closure at FLUXNET sites, *Agric. For. Meteorol.*, *113*(1–4), 223–243.

Woodward, F. I., and M. R. Lomas (2004), Vegetation dynamics — Simulating responses to climatic change, *Biol. Rev.*, *79*(3), 643–670.

Xu, L., and D. D. Baldocchi (2004), Seasonal variation in carbon dioxide exchange over a Mediterranean annual grassland in California, *Agric. For. Meteorol.*, *123*(1–2), 79–96.

Yang, D. W., F. B. Sun, Z. T. Liu, Z. T. Cong, and Z. D. Lei (2006), Interpreting the complementary relationship in non-humid environments based on the Budyko and Penman hypotheses, *Geophys. Res. Lett.*, *33*, L18402, doi:10.1029/2006GL027657.

————————————
D. D. Baldocchi, T. Hehn, S. Ma, and Y. Ryu, Department of Environmental Science, Policy and Management, University of California at Berkeley, 137 Mulford Hall #3114, Berkeley, CA 94720-3114, USA. (yryu@nature.berkeley.edu)